RSC Advances

PAPER

View Article Online
View Journal | View Issue

Cite this: *RSC Adv.*, 2024, **14**, 17195

Chlorine-containing polyacetoxybriarane diterpenoids from the octocoral *Junceella fragilis*†

Hai Nhat Do,‡[ab] Yu-Ta Chen,‡[c] Su-Ying Chien,[d] You-Ying Chen,[b] Mingzi M. Zhang,[e] Lun Kelvin Tsou,[f] Jih-Jung Chen,[g] Zhi-Hong Wen,[a] Yi-Hao Lo,[chi] Li-Guo Zheng *[j] and Ping-Jyun Sung *[abklm]

Received 25th April 2024
Accepted 21st May 2024

DOI: 10.1039/d4ra03062a

rsc.li/rsc-advances

The chemical screening of an octocoral identifed as *Junceella fragilis* has led to the isolation of five chlorinated briarane-type diterpenoids, including three known metabolites, gemmacolide X (**1**), frajunolide I (**2**), and fragilide F (**3**), along with two new analogs, 12α-acetoxyfragilide F (**4**) and 12α-acetoxyjunceellin (**5**). Single-crystal X-ray diffraction analysis was carried out to determine the absolute configurations of **1** and **2**, while the structures of new compounds **4** and **5** were ascertained with 2D NMR experiments. Briaranes **1** and **3**–**5** were active in enhancing alkaline phosphatase (ALP) activity.

1 Introduction

The octocorals belonging to genus *Junceella* (phylum Cnidaria, sub-phylum Anthozoa, class Octocorallia, order Scleralcyonacea, family Ellisellidae),[1] distributed in the shallow waters of the tropical Indo-Pacific Ocean, have been proven to be a rich source of briarane-type diterpenoids with uncommon structures.[2] This study explored further new substances from *Junceella fragilis* (Ridley 1884), collected from waters off the coast of Taiwan, an area with high biodiversity at the intersection of Kuroshio and South China Sea surface currents. The study successfully isolated five chlorinated briaranes, including three known metabolites, gemmacolide X (**1**),[3] frajunolide I (**2**),[4] and fragilide F (**3**),[5] as well as two new analogs, 12α-acetoxyfragilide F (**4**) and 12α-acetoxyjunceellin (**5**) (Fig. 1) and ascertained their structures and ALP activity. The absolute configurations of **1** and **2** were further determined *via* single-

[a]*Department of Marine Biotechnology and Resources, National Sun Yat-sen University, Kaohsiung 804201, Taiwan*
[b]*National Museum of Marine Biology & Aquarium, Pingtung 944401, Taiwan. E-mail: pjsung@nmmba.gov.tw*
[c]*Department of Family Medicine, Zuoying Armed Forces General Hospital, Kaohsiung 813204, Taiwan*
[d]*Instrumentation Center, National Taiwan University, Taipei 106319, Taiwan*
[e]*Institute of Molecular and Genomic Medicine, National Health Research Institutes, Miaoli 350401, Taiwan*
[f]*Institute of Biotechnology and Pharmaceutical Research, National Health Research Institutes, Miaoli 350401, Taiwan*
[g]*Department of Pharmacy, School of Pharmaceutical Sciences, National Yang Ming Chia Tung University, Taipei 112304, Taiwan*
[h]*Shu-Zen Junior College of Medicine and Management, Kaohsiung 821004, Taiwan*
[i]*Institute of Medical Science and Technology, National Sun Yat-sen University, Kaohsiung 804201, Taiwan*
[j]*Doctoral Degree Program in Marine Biotechnology, National Sun Yat-sen University, Kaohsiung 804201, Taiwan. E-mail: t0919928409@gmail.com*
[k]*Chinese Medicine Research and Development Center, China Medical University Hospital, Taichung 404394, Taiwan*
[l]*Graduate Institute of Natural Products, Kaohsiung Medical University, Kaohsiung 807378, Taiwan*
[m]*PhD Program in Pharmaceutical Biotechnology, Fu Jen Catholic University, New Taipei City 242062, Taiwan*

† Electronic supplementary information (ESI) available: HRESIMS, 1D and 2D NMR spectra of **4** and **5**; X-ray crystallographic data of **1** and **2**. CCDC 2323829 and 2326820, respectively. For ESI and crystallographic data in CIF or other electronic format see DOI: https://doi.org/10.1039/d4ra03062a

‡ These authors have contributed equally to this work.

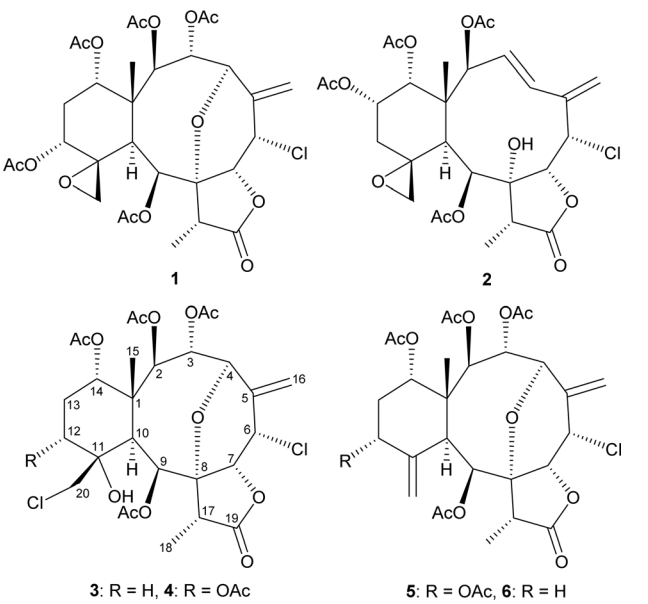

Fig. 1 Structures of gemmacolide X (**1**), frajunolide I (**2**), fragilide F (**3**), 12α-acetoxyfragilide F (**4**), 12α-acetoxyjunceellin (**5**), and junceellin (**6**).

crystal X-ray diffraction analysis with a diffractometer equipped with a copper (Cu Kα) source.

2 Results and discussion

Gemmacolide X (**1**) and frajunolide I (**2**) were originally isolated from the octocorals *Dichotella gemmacea* and *Junceella fragilis*, respectively; and the structures of these two briaranes, including the relative configuration, were elucidated by spectroscopic analysis.[3,4] The absolute configuration of these two compounds was supported in this study by single-crystal X-ray diffraction analysis (Flack parameter $x = 0.000(5)$ for **1** and $-0.002(13)$ for **2**).[6] The ORTEP diagram (Fig. 2) showed that the absolute configuration of stereogenic carbons of **1** and **2** are assigned as 1*R*, 2*R*, 3*R*, 4*R*, 6*S*, 7*R*, 8*R*, 9*S*, 10*S*, 11*R*, 12*R*, 14*S*, 17*R* and 1*S*, 2*S*, 6*S*, 7*R*, 8*R*, 9*S*, 10*S*, 11*R*, 13*S*, 14*R*, 17*R*, respectively.

The (+)-ESIMS of **3** showed sodiated peaks at *m*/*z* 657/659/661 ($[M + Na]^+/[M + 2 + Na]^+/[M + 4 + Na]^+$) (9 : 6 : 1) with a relative intensity suggestive of two chlorine atoms. Strong bands at 3478, 1790, and 1742 cm^{-1} observed in the IR spectrum confirmed the presence of hydroxy, γ-lactone, and ester groups in **3**. It was found that the spectroscopic data of **3** were identical to those of a known briarane, fragilide F, and these two compounds possessed negative optical values ([α] −15 for **3** and [α] −19 for fragilide F);[5] thus, compound **3** was identified as fragilide F.

12α-Acetoxyfragilide F (**4**) was isolated as an amorphous powder and its molecular formula was determined to be $C_{30}H_{38}Cl_2O_{14}$ ($\Omega = 11$) by (+)-HRESIMS at *m*/*z* 715.15302 (calcd for $C_{30}H_{38}Cl_2O_{14}$ + Na, 715.15308). Comparison of the ^{1}H NMR, HSQC, and HMBC data with the molecular formula indicated that there must be an exchangeable proton, requiring the presence of a hydroxy group, and this deduction was supported by a broad absorption in the IR spectrum at 3466 cm^{-1}. The IR spectrum of **4** also showed strong bands at 1791 and 1740 cm^{-1}, consistent with the presence of γ-lactone and ester groups. The presence of an exocyclic olefin was deduced from the signals of an sp^2 methylene carbon at δ_C 119.6 (CH_2-16). Six carbonyl resonances at δ_C 175.2 (C-19), 171.2, 170.2, 170.2, 169.8, and 169.6, confirmed the presence of a γ-lactone and five ester groups; five acetate methyls (δ_H 2.36, 2.07, 2.04, 2.03, and 2.01, each 3H × s) were also observed. From the above NMR data (Table 1), seven degrees of unsaturation were accounted for, and **4** must be tetracyclic.

In addition, a tertiary methyl singlet, a methyl doublet, a pair of aliphatic methylene protons, two aliphatic methine protons, seven oxymethine protons, a downfield methine proton (δ_H 5.04, 1H, ddd, J = 2.4, 2.4, 2.4 Hz, H-6), a pair of low field methylene protons (δ_H 3.52, 1H, d, J = 12.0 Hz; 3.84, 1H, d, J = 12.0 Hz, H-20a/b), and a hydroxy proton (δ_H 3.11, 1*H*, s, OH-11) were observed in the ^{1}H NMR spectrum of **4** (Table 1).

The gross structure of **4** was verified by 2D NMR studies. ^{1}H NMR coupling information in the ^{1}H–^{1}H COSY spectrum of **4** enabled identification of C2–C3–C4, C6–C7, C12–C13–C14, and C17–C18 units, which were assembled with the assistance of an HMBC experiment (Fig. 3). The HMBC between protons and non-protonated carbons of **4**, such as H-2, H-9, H-10, H_3-15/C-1; H-4, H-10, H_3-18/C-8; H-9, H-10, H-20a/C-11; and H-17, H_3-18/C-19, permitted elucidation of the carbon skeleton. An exocyclic double bond attached at C-5 was confirmed by the allylic coupling between H_2-16 and H-6 in the ^{1}H–^{1}H COSY experiment and by the HMBC between H-16a/C-4, C-6; and H-16b/C-6. The ring junction C-15 methyl group was positioned at C-1 from the HMBC between H_3-15/C-1, C-2, C-10, C-14. The presence of a hydroxy group at C-11 was deduced from the HMBC between a hydroxy proton (δ_H 3.11) with C-10 methine (δ_C 41.6). The acetate ester at C-9 was established by a correlation between H-9 (δ_H 6.40) and the acetate carbonyl (δ_C 169.6) observed in the HMBC spectrum. Thus, the remaining four acetoxy groups should be positioned at C-2, C-3, C-12, and C-14, as indicated by the characteristic NMR signal analysis of the oxymethines CH-2 (δ_H 5.48/δ_C 73.1), CH-3 (δ_H 6.19/δ_C 63.8), CH-12 (δ_H 5.52/δ_C 68.6), and CH-14 (δ_H 4.83/δ_C 72.6), respectively, although no HMBC was observed between the oxymethine protons H-2, H-3, H-12, and H-14 and those acetate carbonyls.

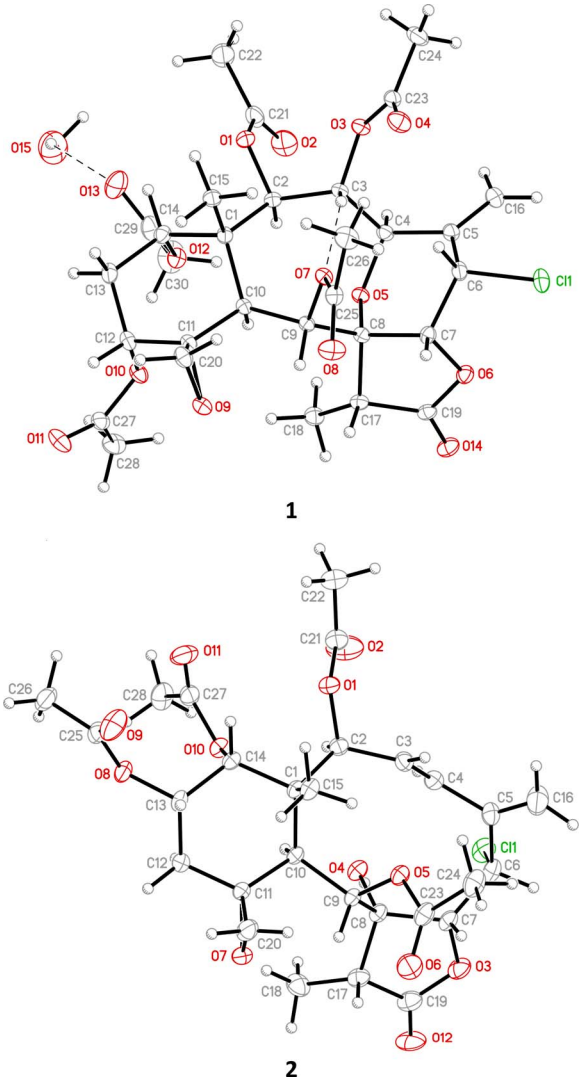

Fig. 2 ORTEP demonstrates the structures of gemmacolide X (**1**) and frajunolide I (**2**).

Table 1 ^{1}H and ^{13}C NMR data for briarane **4**

Position	δ_H[a] (J in Hz)	δ_C[b], Mult.[c]
1		45.1, C
2	5.48 d (6.6)	73.1, CH
3	6.19 dd (10.8, 6.6)	63.8, CH
4	4.47 d (10.8)	78.5, CH
5		N. o.[d]
6	5.04 ddd (2.4, 2.4, 2.4)	53.9, CH
7	4.37 d (2.4)	78.9, CH
8		83.9, C
9	6.40 s	73.2, CH
10	2.99 s	41.6, CH
11		74.6, C
12	5.52 dd (3.0, 3.0)	68.6, CH
13α/β	2.20 ddd (16.8, 3.0, 3.0); 1.97 ddd (16.8, 3.0, 3.0)	26.2, CH_2
14	4.83 dd (3.0, 3.0)	72.6, CH
15	1.30 s	16.4, CH_3
16a/b	5.36 d (2.4); 5.57 d (2.4)	119.6, CH_2
17	2.82 q (7.2)	49.5, CH
18	1.39 d (7.2)	7.2, CH_3
19		175.2, C
20a/b	3.52 d (12.0); 3.84 d (12.0)	48.3, CH_2
OH-11	3.11 s	
Acetoxy groups	2.36 s	21.0, CH_3
		169.6, C
	2.07 s	21.2, CH_3
		171.2, C
	2.04 s	21.0, CH_3
		170.2, C
	2.03 s	20.4, CH_3
		170.2, C
	2.01 s	21.0, CH_3
		169.8, C

[a] Spectra recorded at 600 MHz in $CDCl_3$ at 25 °C. [b] Spectra recorded at 150 MHz in $CDCl_3$ at 25 °C. [c] Data assigned with the assistance of HSQC and HMBC spectra. [d] N. o. = not observed.

The intensity of sodiated molecules $(M + 2 + Na)^+$ and $(M + 4 + Na)^+$ isotope peaks observed in (+)-ESIMS spectrum [$(M + Na)^+ : (M + 2 + Na)^+ : (M + 4 + Na)^+ = 9 : 6 : 1$] were strong evidence of the presence of two chlorine atoms in **4**. The methine unit at δ_C 53.9 was more shielded than that expected for an oxygenated C-atom and was correlated to the methine proton at δ_H 5.04 in the HSQC spectrum and this proton signal was ^{3}J-correlated with H-7 (δ_H 4.37) (J = 2.4 Hz), proving the attachment of a chlorine atom at C-6. In addition, the methylene unit at δ_C 48.3 was also more shielded than that expected for an oxygenated C-atom and was correlated to the methylene protons at δ_H 3.52 and 3.84 in the HSQC spectrum and one of the methylene proton signals (δ_H 3.52, H-20a) exhibited HMBC with C-11 and C-12, proving the attachment of a chloromethyl group at C-11. Furthermore, an HMBC between H-4 (δ_H 4.47) and an oxygenated quaternary carbon at δ_C 83.9 (C-8) suggested the presence of a C-4/8 ether linkage.

The relative stereochemistry of **4** was elucidated by analysis of NOESY correlations and by vicinal ^{1}H–^{1}H proton coupling constants analysis. In the NOESY experiment (Fig. 4), H-10 correlated with H-2, H-9, and H_3-18 indicated that these

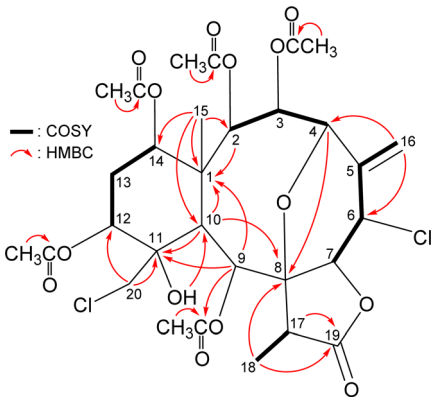

Fig. 3 Key HMBC and COSY correlations of **4**.

protons were situated on the same face; they were assigned as α-protons, as C-15 methyl was β-oriented at C-1 and H_3-15 did not show correlation with H-10. Also, no coupling was found between H-9 and H-10, indicating that the dihedral angle between these two protons was approximately 90°, further confirmed that H-9 had an α-orientation. Due to H-14 proton being correlated with H_3-15, this proton was of a β-orientation at C-14. The C-13 methylene protons displayed identical coupling constants with H-14 (J = 3.0, 3.0 Hz) and H-12 (J = 3.0, 3.0 Hz), respectively, indicating that both H-14 and H-12 should be positioned on the β-equatorial direction in the six-membered ring of **4**.

The oxymethine proton H-3 and one of the chlorinated C-20 methylene protons (δ_H 3.84, H-20b) were found to exhibit responses with H_3-15 but not with H-10, revealing H-3 and C-20 methylene were β-oriented at C-3 and C-11, respectively. H-9 was found to show correlations with H-7, H-17, and one proton of C-20 methylene protons (δ_H 3.52, H-20a). From modeling analysis, H-9 was found to be reasonably close with H-7, H-17, and H-20a and can therefore be placed on the α face in the 10-membered

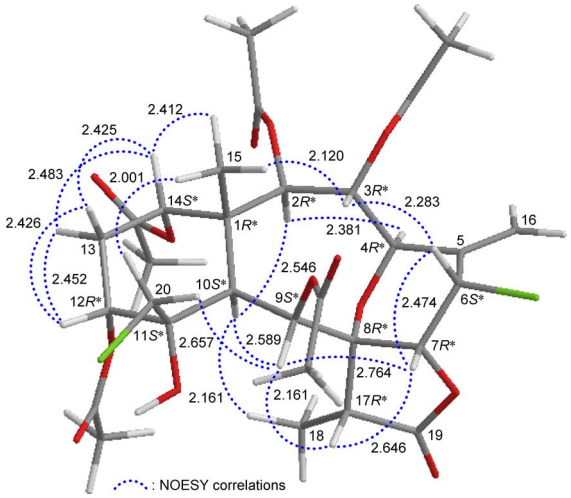

Fig. 4 Stereo-view of **4** (generated by computer modeling) and calculated distances (Å) between selected protons with key NOESY correlations.

Table 2 ^{1}H and ^{13}C NMR data for briarane **5**

Position	δ_H[a] (J in Hz)	δ_C[b], Mult.[c]
1		47.1, C
2	5.55 d (6.6)	72.6, CH
3	6.16 dd (10.8, 6.6)	63.6, CH
4	4.51 d (10.8)	79.0, CH[g]
5		134.1, C
6	5.01 ddd (3.0, 1.8, 1.8)	53.8, CH
7	4.52 d (3.0)	79.0, CH[g]
8		82.8, C
9	5.89 s	77.5, CH
10	3.56 s	39.7, CH
11		144.5, C
12	5.38 dd (3.6, 3.6)[de]	74.8, CH
13α/β	2.19 ddd (16.2, 3.6, 3.0); 1.90 ddd (16.2, 3.6, 2.4)	30.6, CH_2
14	4.93 dd (3.0, 2.4)	73.6, CH
15	1.14 s	14.5, CH_3
16a/b	5.38 d (1.8)[df]; 5.59 d (1.8)[f]	119.7, CH_2
17	2.78 q (7.2)	49.9, CH
18	1.35 d (7.2)	6.9, CH_3
19		173.9, C
20a/b	5.44 s; 5.03 br s	117.5, CH_2
Acetoxy groups	2.34 s	21.2, CH_3
		169.8, C
	2.05 s	21.0, CH_3
		170.7, C
	2.05 s	21.0, CH_3
		169.4, C
	2.01 s	21.0, CH_3
		170.4, C
	2.01 s	21.0, CH_3
		169.6, C

[a] Spectra recorded at 600 MHz in $CDCl_3$ at 25 °C. [b] Spectra recorded at 150 MHz in $CDCl_3$ at 25 °C. [c] Data assigned with the assistance of HSQC and HMBC spectra. [d] Signals overlapped. [e] The coupling pattern and coupling constant for H-12 were assigned by its vicinal couplings with H-13α/β. [f] The coupling pattern and coupling constant for H-16a/b were assigned by their allylic long-range ^{4}J-coupling with H-6. [g] Signals overlapped.

ring and both H-7 and H-17 are β-oriented in the γ-lactone moiety. H-7 exhibited interactions with H-6 and H-17; and H-6 correlated with H-3, indicating that H-7 and H-6 are on the β face. Furthermore, H-4 showed a correlation with H-2; and a large coupling constant was found between H-4 and H-3 (J = 10.8 Hz), indicating the dihedral angle between H-4 and H-3 is approximately 180° and H-4 has an α-orientation at C-4. The above interpretation enables the identification of the relative configuration of all stereogenic centers of **4** as 1*R**, 2*R**, 3*R**, 4*R**, 6*S**, 7*R**, 8*R**, 9*S**, 10*S**, 11*S**, 12*R**, 14*S**, 17*R**. According to the above and comparing the NMR data of **4** with those of the literature, the structure of **4** was similar to that of fragilide F (**3**) (Fig. 1),[5] except for the 12α-proton in **3** was instead of an acetoxy group in **4**. Hence, **4** was found to be the 12α-acetoxy derivative of **3** and named 12α-acetoxyfragilide F.

12α-Acetoxyjunceellin (**5**) was isolated as an amorphous powder. Its (+)-HRESIMS peak was at m/z 663.18121, consistent with the molecular formula $C_{30}H_{37}ClO_{13}$ (calcd for $C_{30}H_{37}ClO_{13}$ + Na, 663.18149) with 12 degrees of unsaturation. The IR spectrum of **5** contained signals of γ-lactone (ν_{max} 1791 cm^{-1}) and ester (ν_{max} 1740 cm^{-1}) functionalities. Analyzing the ^{1}H NMR (Table 2), HSQC, and HMBC spectra of **5** led to the assignment of five acetoxy groups; as well as two exocyclic carbon–carbon double bonds, a γ-lactone moiety, and other 15 carbon signals (Table 2).

The carbon skeleton of **5** was fully established by following correlations observed in the ^{1}H–^{1}H COSY and HMBC spectra (Fig. 5). The oxymethine protons H-3 (δ_H 6.16), H-9 (δ_H 5.89), and H-2 (δ_H 5.55) showed HMBC to the acetate carbonyls at δ_C 169.6, 169.8, and 170.4, confirmed the position of acetoxy groups at C-3, C-9, and C-2, respectively. Evaluated on the NMR chemical shifts of oxymethines CH-12 (δ_H 5.38/δ_C 74.8) and CH-14 (δ_H 4.93/δ_C 73.6), the remaining acetoxy groups should be positioned at C-12 and C-14, respectively.

The relative stereochemistry of **5** was established by analyzing the NOESY information in combination with the computer-generated model structure. We have noticed that all naturally-occurring briaranes possess a β-Me-15 placed at C-1 and have an α-orientation of H-10. In the NOESY spectrum (Fig. 6), H-10 showed correlations with H-2, H-9, and H_3-18; H_3-15 was correlated with H-3, H-14, and one of the C-13 methylene protons (δ_H 1.90, H-13β); and H-13β was correlated with H-12, proving the α-orientation of OAc-3, OAc-12, and OAc-14; and β-orientation of OAc-2 and OAc-9. H-3 exhibited an interaction with H-6; and H-6 correlated with H-7, indicating that H-6 and H-7 are on the β face. Furthermore, H-4 showed a correlation with H-2; and a large coupling constant was found between H-4 and H-3 (J = 10.8 Hz), indicating the dihedral angle between H-4 and H-3 is approximately 180° and H-4 has an α-orientation at C-4. Additionally, there was a correlation between H-7 and H-17, suggesting that H-17 is situated on the β face in the γ-lactone moiety. The above interpretation enables the identification of the relative configuration of all stereogenic centers of **5** as 1*R**, 2*R**, 3*R**, 4*R**, 6*S**, 7*R**, 8*R**, 9*S**, 10*S**, 12*R**, 14*S**, 17*R**. It was found that the NMR signals of **5** were similar to those of a known briarane, junceellin (**6**),[7,8] except that the signals corresponding to the α-proton at C-12 in **6** were replaced by signals for an acetoxy group in **5**. Thus, **5** was found to be the 12α-acetoxy derivative of **6** and named 12α-acetoxyjunceellin.

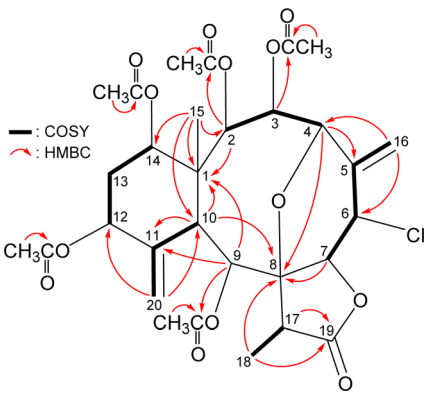

Fig. 5 Key HMBC and COSY correlations of **5**.

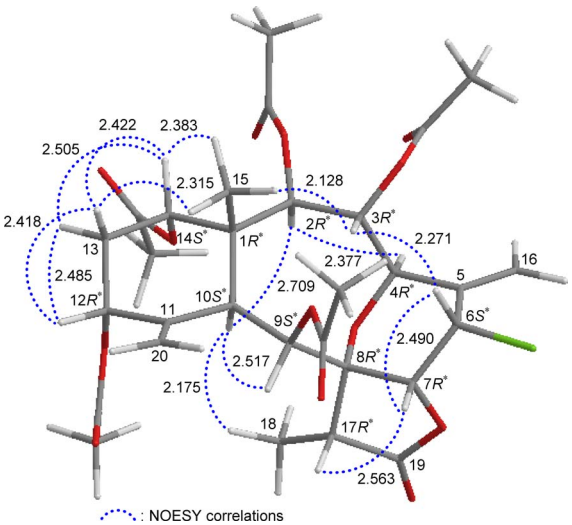

Fig. 6 Stereo-view of **5** (generated by computer modeling) and calculated distances (Å) between selected protons with key NOESY correlations.

Table 3 The evaluation of ALP activity ensued subsequent to subjecting MG63 cells to briaranes **1**–**5** at concentration of 10 μM or 100 μM rutin (utilized as a positive control) for[a] 72 h

Compounds	ALP activity (king unit per mg prot.)
1	4.2 ± 1.0**
2	2.9 ± 1.1**
3	6.6 ± 0.2***
4	5.8 ± 0.5***
5	4.8 ± 0.7***
Rutin	3.1 ± 0.2
Control	−5.0 ± 0.5

[a] Data are expressed with the mean standard error of the mean (SEM) (n = 3). The significance was determined with Student's t-test. **p < 0.01, ***p < 0.001 and comparison with untreated cells.

As briaranes **4** and **5**, in addition to **1** and **2**, were isolated from the same target organism, *J. fragilis*, it is reasonable to assume on biogenetic grounds that briaranes **4** and **5** have the same absolute configuration as **1** and **2**. Therefore, the absolute configurations of **4** and **5** were suggested to be (1*R*, 2*R*, 3*R*, 4*R*, 6*S*, 7*R*, 8*R*, 9*S*, 10*S*, 11*S*, 12*R*, 14*S*, 17*R*) and (1*R*, 2*R*, 3*R*, 4*R*, 6*S*, 7*R*, 8*R*, 9*S*, 10*S*, 12*R*, 14*S*, 17*R*), respectively.

Previous studies have found briarane-type natural products to be a natural remedy for osteoclastogenic disease.[9,10] *Via* an ALP ELISA assay with MG63 human mesenchymal stem cells (Table 3), the study found that briaranes **1** and **3**–**5** were active in enhancing ALP activity at a concentration of 10 μM.

3 Conclusions

The octocorals belonging to the genus *Junceella* have demonstrated a wide structural diversity of briarane diterpenoids with various pharmacological properties.[2] In our ongoing research on *J. fragilis*, we isolated five chlorinated briaranes, including two previously undiscovered briaranes: 12α-acetoxyfragilide F (**4**) and 12α-acetoxyjunceellin (**5**). Three known analogs were also identified: gemmacolidex (**1**),[3] frajunolide I (**2**),[4] and fragilide F (**3**).[5] The structures, including the absolute configurations, of **1** and **2** were further established through single-crystal X-ray diffraction analysis. For compounds **4** and **5**, their structures were confirmed using various spectroscopic techniques, particularly 2D NMR experiments and comparison with existing literature data. Briaranes **1** and **3**–**5** were active in enhancing ALP activity.

4 Experimental

4.1 General experimental procedures

Optical rotation values were measured using a JASCO P-1010 digital polarimeter. IR spectra were obtained with a Thermo Scientific Nicolet iS5 FT-IR spectrophotometer. NMR spectra were recorded on a 600 MHz Jeol ECZ NMR spectrometer using the residual $CHCl_3$ (δ_H 7.26 ppm) and $CDCl_3$ (δ_C 77.0 ppm) as internal standards for ^1H and ^{13}C NMR, respectively; coupling constants (J) are presented in Hertz (Hz). The ESIMS and HRESIMS spectra were ascertained with Thermo Fisher orbitrap Exploris 120 mass spectrometer equipped with an ESI ion source in positive ionization mode. The extracted samples were separated *via* column chromatography with silica gel (particle size, 230–400 mesh; Merck). TLC was performed on plates precoated with silica gel 60 (DC-Fertigfolien Alugram Xtra SIL G/UV_{254}, layer thickness 0.20 mm, Macherey-Nagel) and RP-18 F_{254}S (layer thickness 0.16–0.20 mm, Merck), and visualization of the TLC plates was conducted using an aqueous solution of 10% H_2SO_4, subsequently to be heated to show the spots of signals. Reverse-phase HPLC (RP-HPLC) separation was carried out with a system containing a pump (Hitachi, model L-7110) with a photo-diode array detector (Hitachi, model L-2400), equipped with a reverse-phase column (Luna, 5 μm, C18(2) 100 Å, 250 × 21.2 mm). Normal-phase HPLC (NP-HPLC) separation was carried out with a system containing a pump (Hitachi, model L-5110), equipped with a normal-phase column (Galaksil, EF-SiO_2, 5 μm 120 Å, 250 × 10 mm).

4.2 Animal material

Specimen of *J. fragilis* was collected manually *via* SCUBA diving off the coast of Southern Taiwan in 2012. A voucher specimen was deposited at the National Museum of Marine Biology & Aquarium, Taiwan. To identify the species, we compared its physical characteristics and microscopic images of the coral sclerites with those mentioned in previous studies.[1,11–13]

4.3 Extraction and isolation

The freeze-dried specimen (wet/dry weight = 6.01/2.39 kg) was sliced and treated with a 1 : 1 mixture solvent of MeOH and CH_2Cl_2 at room temperature to produce crude extract weighing 140.1 g, which was then subjected to liquid–liquid partition between EtOAc and H_2O. The EtOAc phase (19.2 g) was applied to a silica gel column chromatography (Si. C. C.). Elution was

carried out with a gradient solvent system containing *n*-hexane, followed by increasing polarity mixtures of *n*-hexane and EtOAc, pure acetone, and pure methanol for use as eluting solvents. The process yielded 13 fractions A–M. Fraction D was chromatographed with NP-HPLC *via* an isocratic solvent system, *n*-hexane/acetone mixture (6 : 1). The process yielded 7 fractions D1–D7. Fraction D6 was separated with NP-HPLC *via* an isocratic solvent system, DCM/acetone mixture (18 : 1). The process yielded 3 fractions D6A–D6C. Fraction D6A was purified with RP-HPLC *via* an isocratic solvent system, ACN/H_2O mixture (60 : 40; flow rate = 3 mL min^{-1}), to afford **3** (0.4 mg). Fraction E was chromatographed with Si. C.C. and eluted with an isocratic solvent system, DCM/acetone mixture (10 : 1). The process yielded 8 fractions E1–E8. Fraction E2 was separated by NP-HPLC *via* an isocratic solvent system, *n*-hexane/EtOAC mixture (2 : 1) to obtain 5 fractions E2A–E2E. Fraction E2E was purified by RP-HPLC with an isocratic solvent system, ACN/H_2O mixture (50 : 50; flow rate = 3 mL min^{-1}), to obtain **2** (0.3 mg). Fraction E2D was purified by RP-HPLC with an isocratic solvent system, ACN/H_2O mixture (60 : 40; flow rate = 3 mL min^{-1}), to obtain **5** (0.4 mg). Fraction F was separated on Si. C. C. with an isocratic solvent system, DCM/acetone mixture (15 : 1). The process yielded 8 fractions F1–F8. Fraction F4 was separated Si C. C. and eluted with DCM/EtOAc mixture (20 : 1) to yield 6 fraction F4A–F4F. Fraction F4E was purified by RP-HPLC with an isocratic solvent system, MeOH/H_2O mixture (70 : 30; flow rate = 3 mL min^{-1}) to obtain **1** (0.8 mg) and **4** (0.4 mg), respectively.

4.4 Structural characterization of undescribed compounds

4.4.1 12α-Acetoxyfragilide F (4). Amorphous powder; [α] −39 (*c* 0.02, $CHCl_3$); IR (KBr) ν_{max} 3466, 1791, 1740 cm^{-1}; ^1H (600 MHz, $CDCl_3$) and ^{13}C NMR (150 MHz, $CDCl_3$) data (see Table 1); ESIMS: *m*/*z* 715 $[M + Na]^+$, 717 $[M + 2 + Na]^+$, 719 $[M + 4 + Na]^+$; HRESIMS: *m*/*z* 715.15302 (calcd for $C_{30}H_{38}Cl_2O_{14}$ + Na, 715.15308).

4.4.2 12α-Acetoxyjunceellin (5). Amorphous powder; [α] +275 (*c* 0.02, $CHCl_3$); IR (KBr) ν_{max} 1791, 1740 cm^{-1}; ^1H (600 MHz, $CDCl_3$) and ^{13}C NMR (150 MHz, $CDCl_3$) data (see Table 2); ESIMS: *m*/*z* 663 $[M + Na]^+$, 665 $[M + 2 + Na]^+$; HRESIMS: *m*/*z* 663.18121 (calcd for $C_{30}H_{37}ClO_{13}$ + Na, 663.18149).

4.5 Single-crystal X-ray crystallography of gemmacolide X (1)

Suitable colorless prisms of **1** were obtained from a solution of MeOH. The crystal (0.363 × 0.235 × 0.198 mm^3) was identified as being of the orthorhombic system, space group $P2_12_12_1$ (#19),[14] with a = 12.2945(2) Å, b = 12.4454(2) Å, c = 22.2997(4) Å, V = 3412.08(10) $Å^3$, Z = 4, D_{calcd} = 1.297 Mg m^{-3} and λ (Cu Kα) = 1.54178 Å. Intensity data were obtained on a crystal diffractometer (Bruker, model: D8 Venture) up to a θ_{max} of 68.349°. All measurement data of 34 394 reflections were collected, of which 6232 were independent. The structure was solved by direct methods and refined by a full-matrix least-squares on F^2 procedure.[15,16] The refined structural model converged to a final R_1 = 0.0292; wR_2 = 0.0758 for 5969 observed reflections [$I > 2\sigma(I)$] and 425 variable parameters; and the absolute configuration was established from the Flack parameter x = 0.000(5).[6,17,18] Crystallographic data for the structure of gemmacolide X (**1**) were submitted to the Cambridge Crystallographic Data Center (CCDC) with ESI publication number CCDC 2323829 (data can be obtained from the CCDC website at https://www.ccdc.cam.ac.uk/conts/retrieving.html).

4.6 Single-crystal X-ray crystallography of frajunolide I (2)

Suitable colorless prisms of **2** were obtained from a solution of MeOH. The crystal (0.191 × 0.102 × 0.049 mm^3) was identified as being of the hexagonal system, space group $P6_1$ (#169),[14] with $a = b$ = 22.8317(3) Å, c = 10.2937(2) Å, V = 4647.06(15) $Å^3$, Z = 6, D_{calcd} = 1.284 Mg m^{-3} and λ (Cu Kα) = 1.54178 Å. Intensity data were obtained on a crystal diffractometer (Bruker, model: D8 Venture) up to a θ_{max} of 74.402°. All measurement data of 47 636 reflections were collected, of which 6221 were independent. The structure was solved by direct methods and refined by a full-matrix least-squares on F^2 procedure.[15,16] The refined structural model converged to a final R_1 = 0.0358; wR_2 = 0.0960 for 5789 observed reflections [$I > 2\sigma(I)$] and 377 variable parameters; and the absolute configuration was established from the Flack parameter x = −0.002(13).[6,17,18] Crystallographic data for the structure of frajunolide I (**2**) were submitted to CCDC with ESI publication number CCDC 2326820 (data can be obtained from the CCDC website at https://www.ccdc.cam.ac.uk/conts/retrieving.html).

4.7 Alkaline phosphatase (ALP) activity assay

The ALP assay was released to assess the activity of compounds **1**–**5** from MG63 human mesenchymal stem cells, in line with suggestion of previous studies.[19]

Author contributions

Hai Nhat Do and Yu-Ta Chen: methodology, software, analysis, investigation, data curation, original draft writing. Su-Ying Chien: analysis, investigation. You-Ying Chen: investigation. Mingzi M. Zhang, Lun Kelvin Tsou, Jih-Jung Chen, Zhi-Hong Wen, and Yi-Hao Lo: methodology, software, analysis. Li-Guo Zheng and Ping-Jyun Sung: conceptualization, resources, draft review & editing, visualization, supervision, project administration, fundraising.

Conflicts of interest

There are no conflicts to declare.

Acknowledgements

The authors would like to thank Ms. Hsiao-Ching Yu and Chao-Lien Ho, of the High Valued Instrument Center, National Sun Yat-sen University, for the mass (MS 006500) and NMR (NMR 001100) spectra (NSTC 112-2740-M-110-002), and to the Instrumentation Center, National Taiwan University, for providing X-ray facilities (NSTC 112-2740-M-002-006, XRD 000200). This research has been principally supported by grants from the National Museum of Marine Biology & Aquarium, the National

Science and Technology Council (NSTC 111-2320-B-291-001, 112-2320-B-291-001, and 112-2811-B-291-002) and the Zuoying Armed Forces General Hospital (KAFGH-ZY-A-112020), Taiwan, awarded to Yu-Ta Chen and Ping-Jyun Sung. All funding is gratefully acknowledged.

Notes and references

1 C. S. McFadden, L. P. van Ofwegen and A. M. Quattrini, Revisionary systematics of octocorallia (Cnidaria: Anthozoa) guided by phylogenomics, *Bull. Soc. Syst. Biol.*, 2022, **1**, 8735.

2 H.-M. Chung, Y.-C. Wang, C.-C. Tseng, N.-F. Chen, Z.-H. Wen, L.-S. Fang, T.-L. Hwang, Y.-C. Wu and P.-J. Sung, Natural product chemistry of gorgonian corals of genus *Junceella*–part III, *Mar. Drugs*, 2018, **16**, 339.

3 C. Li, M.-P. La, H. Tang, W.-H. Pan, P. Sun, K. Krohn, Y.-H. Yi, L. Li and W. Zhang, Bioactive briarane diterpenoids from the South China Sea gorgonian *Dichotella gemmacea*, *Bioorg. Med. Chem. Lett.*, 2012, **22**, 4368–4372.

4 C.-C. Liaw, Y.-C. Shen, Y.-S. Lin, T.-L. Hwang, Y.-H. Kuo and A. T. Khalil, Frajunolides E–K, briarane diterpenes from *Junceella fragilis*, *J. Nat. Prod.*, 2008, **71**, 1551–1556.

5 P.-J. Sung, S.-H. Wang, M. Y. Chiang, Y.-D. Su, Y.-C. Chang, W.-P. Hu, C.-Y. Tai and C.-Y. Liu, Discovery of new chlorinated briaranes from *Junceella fragilis*, *Bull. Chem. Soc. Jpn.*, 2009, **82**, 1426–1432.

6 S. Parsons, H. D. Flack and T. Wagner, Use of intensity quotients and differences in absolute structure refinement, *Acta Crystallogr.*, 2013, **B69**, 249–259.

7 Y. Lin and K. Long, Studies of the chemical constituents of the Chinese gorgonian (IV)—Junceellin, a new chlorine-containing diterpenoid from *Junceella squamata*, *Zhongshan Daxue Xuebao, Ziran Kexueban Acta Sci. Nat. Univ. Sunyatseni*, 1983, **22**(2), 46–51.

8 J. Shin, M. Park and W. Fenical, The junceellolides, new anti-inflammatory diterpenoids of the briarane class from the Chinese gorgonian *Junceella fragilis*, *Tetrahedron*, 1989, **45**, 1633–1638.

9 Y.-Y. Lin, Y.-H. Jean, H.-P. Lee, S.-C. Lin, C.-Y. Pan, W.-F. Chen, S.-F. Wu, J.-H. Su, K.-H. Tsui, J.-H. Sheu, P.-J. Sung and Z.-H. Wen, Excavatolide B attenuates rheumatoid arthritis through the Inhibition of osteoclastogenesis, *Mar. Drugs*, 2017, **15**, 9.

10 X. Qi, X. Zhang, J. Meng, J. Wu, W. Cheng, J. Huang and W. Lin, Briarane-type diterpenoids, the inhibitors of osteoclast formation by interrupting Keap1-Nrf2 interaction and activating Nrf2 pathway, *Eur. J. Med. Chem.*, 2023, **246**, 114948.

11 C.-F. Dai, *Octocoral Fauna of Taiwan, Ocean Center*, National Taiwan University, Taipei, Taiwan, 2019, pp. 636–637.

12 C.-F. Dai and C.-H. Chin, *Octocoral Fauna of Kenting National Park*, Kenting National Park Headquarters, Kenting, Pingtung, 2019, pp. 492–493.

13 C.-F. Dai, *Corals of Taiwan, Octocorallia*, Owl Publishing House Co., Ltd, Taipei, 2022, vol. 2, p. 381.

14 D. Hestenes and J. W. Holt, Crystallographic space groups in geometric algebra, *J. Math. Phys.*, 2007, **48**, 023514.

15 G. M. Sheldrick, Crystal structure refinement with SHELXL, *Acta Crystallogr.*, 2015, **C71**, 3–8.

16 G. M. Sheldrick, SHELXT-Integrated space-group and crystal-structure determination, *Acta Crystallogr.*, 2015, **A71**, 3–8.

17 H. D. Flack, On enantiomorph-polarity estimation, *Acta Crystallogr.*, 1983, **A39**, 876–881.

18 H. D. Flack and G. Bernardinelli, Absolute structure and absolute configuration, *Acta Crystallogr.*, 1999, **A55**, 908–915.

19 Y. Wang, B. Kong, X. Chen, R. Liu, Y. Zhao, Z. Gu and Q. Jiang, BMSC exosome-enriched acellular fish scale scaffolds promote bone regeneration, *J. Nanobiotechnol.*, 2022, **20**, 444.